Electronic supplementary information

Boron Nitride Aerogels Consisting of Varied Superstructures

Jingjing Pan[ab] and Jingyang Wang[a*]

[a]Shenyang National Laboratory for Materials Science, Institute of Metal Research, Chinese Academy of Sciences, Shenyang 110016, China. Correspondence：jywang@imr.ac.cn

[b]School of Materials Science and Engineering, University of Science and Technology of China, Hefei 230026, China.

Additional explanations about the multilevel assembly scheme

Given the unfamiliarity of multilevel assembly scheme to readers, we present here additional explanations about this scheme.

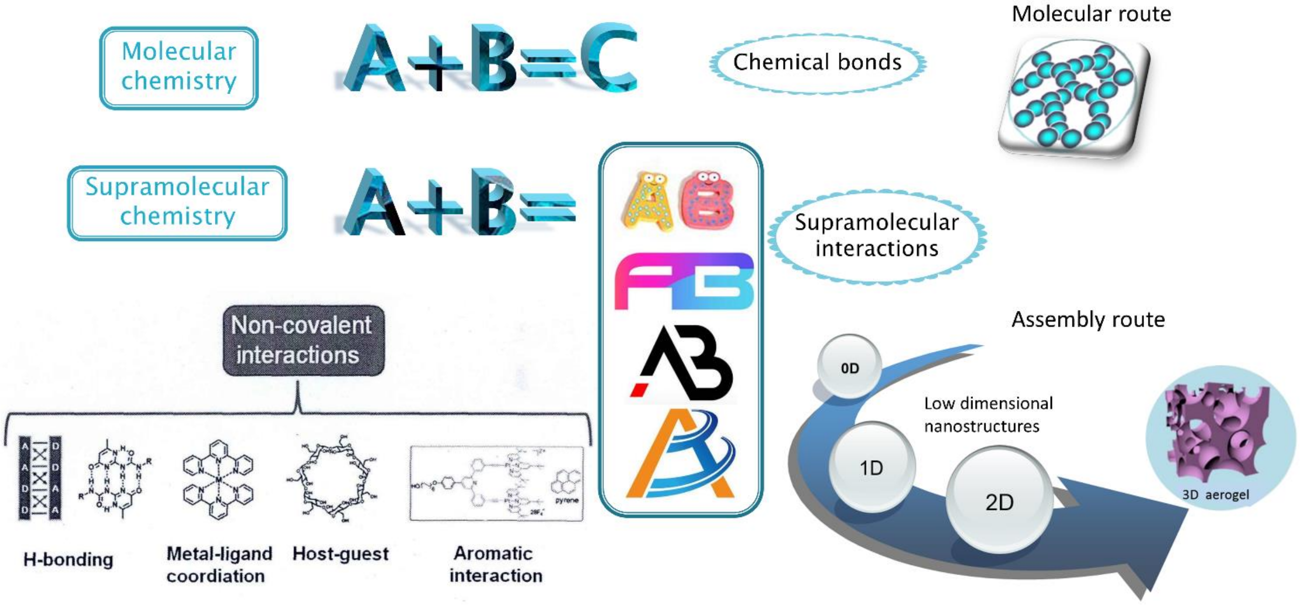

Figure S1* Illustration of the molecular chemistry and supramolecular chemistry and their relationship with the existing aerogel fabrication routes.

The traditional molecular route involves molecular precursors which are converted to wet gels by chemical reactions. Because of the formation of new chemical bonds, the integrate aerogel is "fixed" once formed. In this case, the possibility for microstructure tailoring is limited. Even though it's possible to tailor microstructures via making precursors react with directing agents, e.g. using TEOS modified with silica coupling agents for SiO_2 aerogel fabrication, this approach is only applicable for several constituents. The first-reported BN aerogel derived from trichloroborazene[1], technically speaking, may also be bestowed with varied structures by making raw trichloroboroazene react with some directing agents. But the safety concern and inefficiency impedes the practical applications. Overall, the molecular route is within the scope of molecular chemistry, which deals with the issue of "A+B=C". Molecular chemistry per se gives limited freedom for the realization of varied microstructures.

But what happened when the assembly route was introduced to aerogel field? The ready-made nanostructures were used as building blocks and transformed into integrate aerogels by assembly process, the driving forces for which was not chemical reactions between precursors but the supramolecular interactions. In this respect, the introduction of the assembly route in the late 1990s could be considered as a show in aerogel field made by supramolecular chemistry, which deals with the issue of “A+B=A-B”. Supramolecular chemistry offers great scope for microstructure tailoring given the versatility of non-covalent interactions.

In the classic assembly route, the building blocks (A and B) are ready-made nanostructures, which could be assembled into varied aerogels. Besides the versatile non-covalent interactions, the diverse choices of nanostructures also contribute to the varied microstructures. However, the current assembly route is confronted with some challenges posed by BN. The direct exploitation of BN nanostructures for aerogel fabrication are limited by the lack of controllable surface groups and the difficulty in scalable and efficient production of BN dots, nanotubes etc.

Multilevel assembly here is a modified assembly route. It also exploits the advantage of supramolecular chemistry, whereas the building blocks (A and B) here are not the ready-made nanostructures, such as BN dots or BN nanotubes but molecules that assemble into different motifs at first and then be converted to final aerogels. It avoids the trouble during directly assembling inert BN nanostructures to 3D aerogels but also offers great freedom for microstructure tailoring. This scheme could be summarized as A+B=A-B→C. In this case, the origin of the varied microstructures still lies in the versatility of supramolecular chemistry. Different from the classic assembly route, herein the fabrication of target building blocks and the processing of aerogel are not apart but synchronous, therefore the control over the performance of the resultant aerogels could be exerted by the roots. (In the classic assembly route, the quality of the resultant aerogels relies heavily on the ready-made building blocks (used as received) and the modulation of overall properties mainly counts on post procedures and could hardly be realized by the roots.)

In the classic assembly routes, diverse choices of nanostructures and supramolecular interactions contribute to the versatile microstructures. As for the multilevel assembly scheme, it could be anticipated that the alteration of building molecules and non-covalent interactions could also give rise to varied structures. In this work, three types of molecules were selected and the non-covalent interaction is hydrogen bonds. While the toolbox in supramolecular chemistry is far larger than we have exploited, there may be more possibilities worthy of further explorations.

Table S1* Comparison of molecular route, assembly route and multilevel assembly route

	Molecular route	Assembly route	Multilevel assembly route
The scope for microstructure tailoring	Limited	Great	Great
The control over the performance of the resultant aerogels	Can be exerted by the roots	Limited	Can be exerted by the roots
Potential for high temperature applications	Great	Limited	Great

Experiments

Chemicals

Boric acid (AR), melamine (CP) and were purchased from Sinopharm Chemical Reagent Co., Ltd. Acetoguanamine (98%) was purchased from Shanghai Macklin Biochemical Co., Ltd. Distilled water was provided by Tianzhiyuan Company. All reagents in this work were used without further purification.

Preparation of BN aerogels

In one case, melamine (M)/acetoguanamine (M*) and boric acid (B) were used as molecular building blocks. M/M* and B at different molar ratio (1:2, 1:4, 1:6) were dissolved in distilled water (The total concentration was kept at 30 mg/ml) and stirred at 90℃ for 1h. In the other case, melamine (M), acetoguanamine (M*) and boric acid (B) were dissolved in distilled water. And the molar ratio of M, M* and B were kept at 1:1:2, 1:1:6 and 1:1:10, respectively. Other experimental parameters and procedures were the same as those in the first case. Detailed amount of the raw materials in both cases is given in **Table S1**.The above mixtures were then poured into different containers and cooled down under room temperature (RT). A series of white supramolecular gels were obtained and subsequently put into the freeze dryer (SCIENTZ-10N). After a 24-hour pre-frozen treatment at -35℃ and a 48-hour drying process at RT, the samples were then heated to 1400℃ under argon flow in a tube furnace. The heating rate and soaking time are 5℃/min and 4h, respectively. The final BN aerogels were then obtained.

Preparation of BN plates

To confirm the influence of microstructure on the wettability of BN aerogels, the as-obtained aerogels (BN aerogels derived from M:B=1:6, M:M*:B=1:1:6, M:M*:B=1:1:10) were pressed into flat plates. In each time, 250 mg sample was put into a mold with a diameter of 20mm, and the force applied was 30kN.

Characterization

X-ray diffraction (XRD) experiments were performed on X-ray diffractometer (Rigaku D/max-2400, Japan) with Cu Kα irradiation. FTIR spectra was collected on FTIR Spectrometer (PerkinElmer Spectrum One, USA) and the spectrum resolution was set at 4 cm^{-1}. SEM observations were performed by using scanning electron microscope (LEO Supra 35, Germany). TEM studies were conducted on transmission electron microscope (FEI Tecnai G^2 F20, Netherlands). XPS spectra were obtained on X-ray photoelectron spectrometer (ESCALAB, Thermo VG, USA) and the data was analyzed by using XPSPEAK software. N_2 adsorption test was conducted on Micromeritics ASAP 2020. Contact angle was measured on contact angle tester (Dataphysics OCA20, USA) under room temperature using water droplets of 5μL as indicator.

Supplementary tables and figures

Table S1. Details about the amount of starting materials in different cases.

Total concentration	**Total volume**	**Molar ratio M: M*: B**	**Mass of M**	**Mass of M***	**Mass of B**
30 mg/ml	100ml	1:0:2	1.5148 g	0 g	1.4852 g
30 mg/ml	100ml	1:0:4	1.0132 g	0 g	1.9868 g
30 mg/ml	100ml	1:0:6	0.7611 g	0 g	2.2389 g
30 mg/ml	100ml	0:1:2	0 g	1.5089 g	1.4911 g
30 mg/ml	100ml	0:1:4	0 g	1.0079 g	1.9921 g
30 mg/ml	100ml	0:1:6	0 g	0.7567 g	2.2433 g
30 mg/ml	100ml	1:1:2	1.0092 g	1.0013 g	0.9895 g
30 mg/ml	100ml	1:1:6	0.6081 g	0.6033 g	1.7886 g
30 mg/ml	100ml	1:1:10	0.4351 g	0.4317 g	2.1332 g

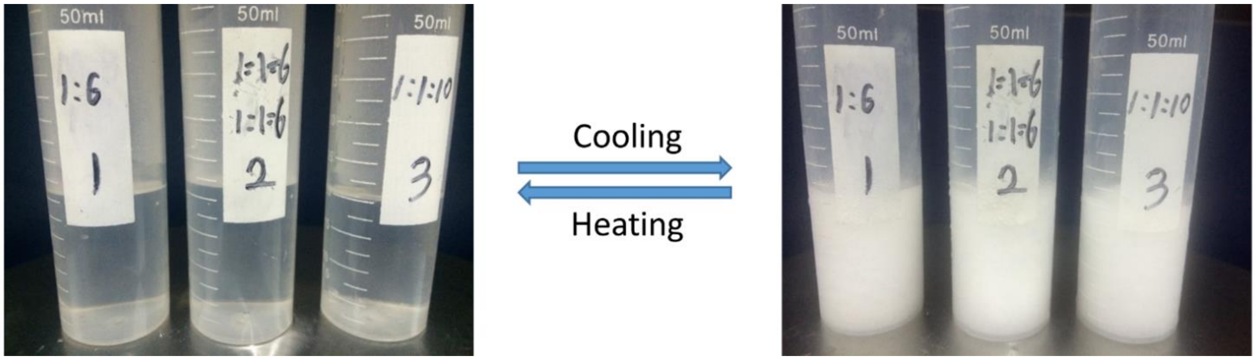

Fig. S1 The reversible transition of solution and gel states.

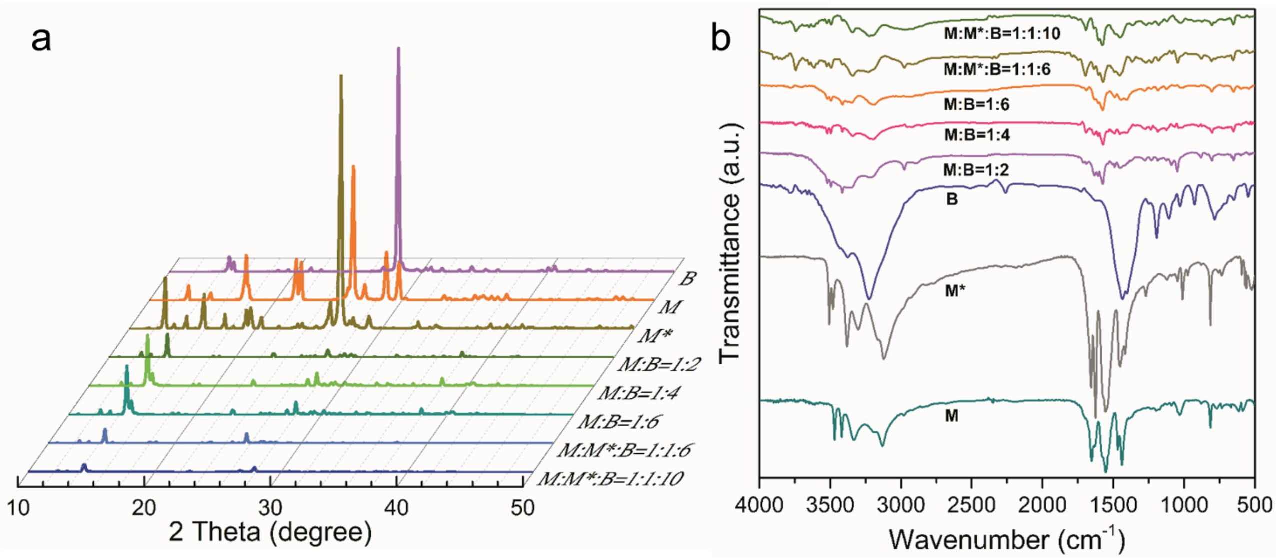

Fig. S2 (a) XRD patterns and (b) FTIR spectra of the supramolecular gels.

With fascinating H-bonding interaction sites, melamine (1,3,5-Triazine) and its analogous derivatives are active members in supramolecular chemistry which enables the formation of complex architectures via assembly process driven by non-covalent interactions[2]. It has long been recognized that melamine and boric acid are able to form supramolecular assemblies via H-bond interactions. Besides melamine, acetoguanamine (6-Methyl-1,3,5-triazine-2,4-diamine) is also involved here and it's believed to have the similar power as melamine. The supramolecular gels obtained at two cases were characterized by using XRD and FTIR methods. As shown in Figure S1(a), the diffraction peaks for pure molecular building blocks, i.e. melamine, acetoguanamine and boric acid are sharp and intense, whereas the dried supramolecular gels show obviously weak peaks and the patterns are distinctly different from those of pure substances, implying that molecular building blocks have transformed into supramolecular aggregates by interacting with each other. The FTIR spectra further confirm the interaction between different molecules. Previous research has revealed that the formation of M•2B adduct is led by hydrogen-bonding interaction[3], which can also be supported by the results in our work. As Figure S1(b) displays, sharp peaks that correspond to the vibration mode of —NH_2 in M and M* are at around 3400—3550 cm^{-1}. The broad peak of B at 3225 cm^{-1} can be attributed to stretching mode of -OH[4]. It's clear that after the supramolecular assembly process, these peaks become broadened and the relative intensity decreases, indicating the formation of hydrogen bonds between them. This result is in accord with the previous studies about M•2B supramolecules, which were claimed as "hydrogen-bonded adduct"[5].

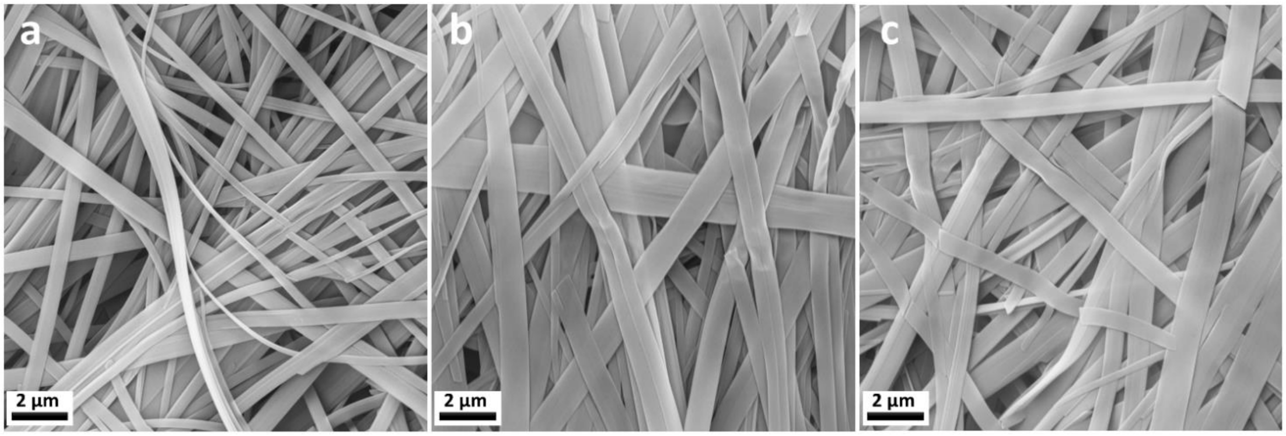

Fig. S3 SEM images of the supramolecular gels obtained at M: B=1:2 (a), M:B=1:4 (b), M:B=1:6 (c).

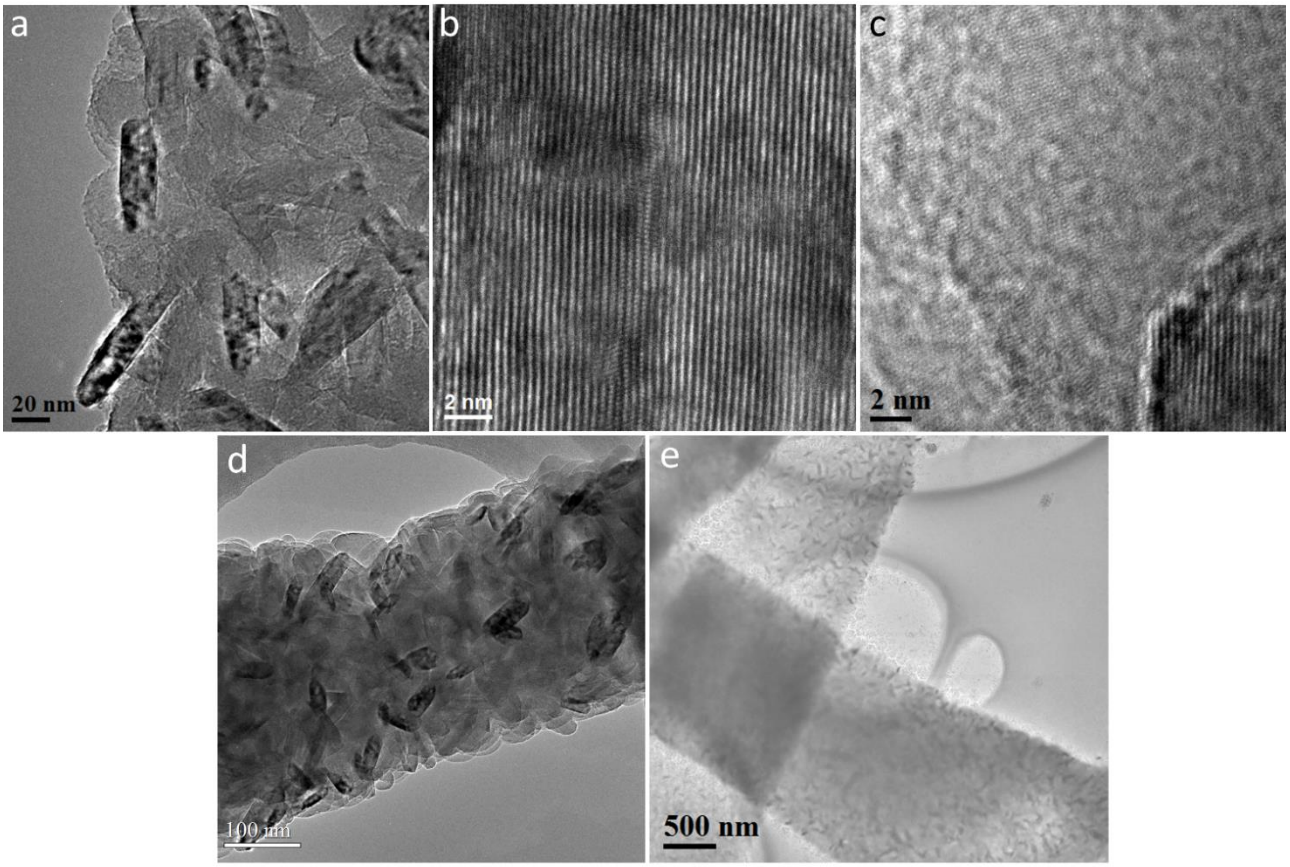

Fig. S4 TEM images of BN aerogel derived from M:B=1:6. (a)-(c) supplement the images shown in main text. (d) and (e) are additional areas in the same sample, corresponding to thick and thin nanoribbons, respectively.

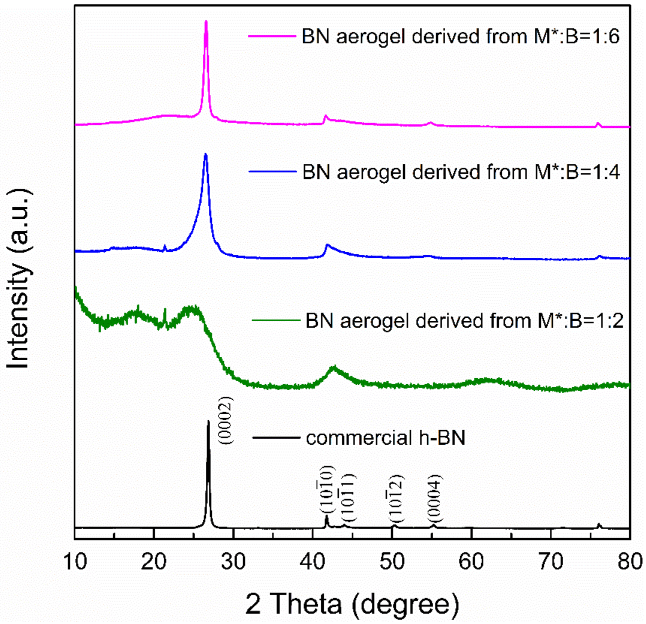

Fig. S5 XRD patterns of the resultant aerogels derived from M* and B at different molar ratio

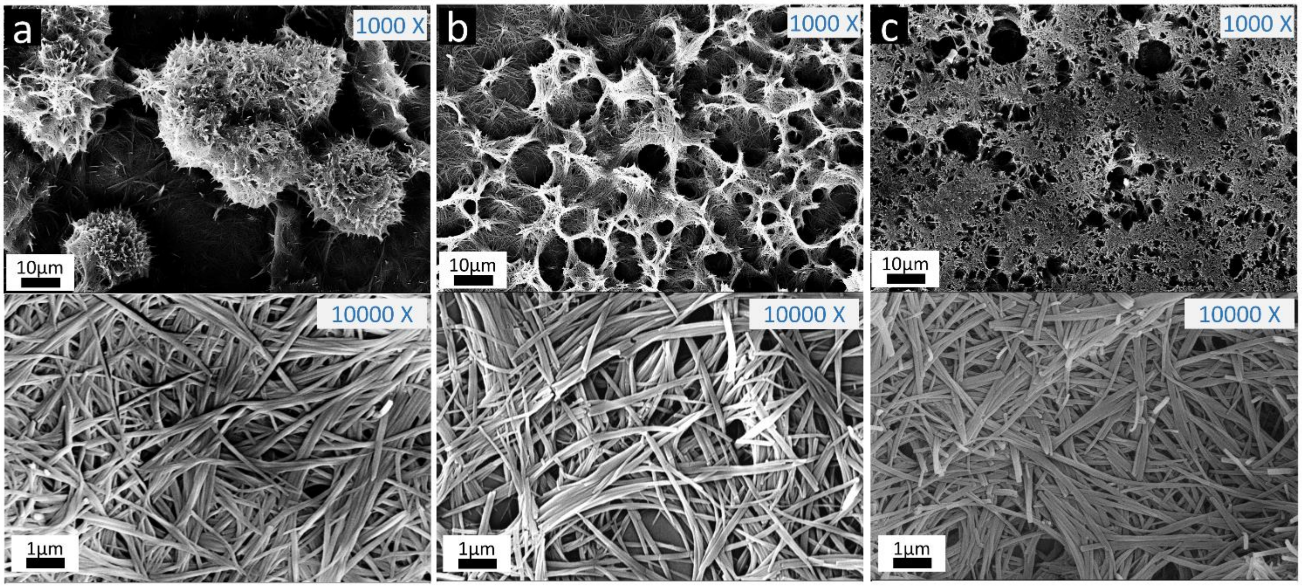

Fig. S6 SEM images of the supramolecular gels obtained at M*: B=1:2 (a), M*: B=1:4 (b), M*: B=1:6 (c). Notes for readers: If you re-perform this experiment in your lab and put the samples under SEM observations, you may get confused about the phenomena that in sample b, there are some areas sharing similar micromorphology as those in sample a; likewise, in sample c, you could also observe areas with similar micromorphologies as sample b and sample a. In this case, “tendency” is more important than “absolute result”; therefore, we need to pay more attention to the evolvement process rather than the single samples.

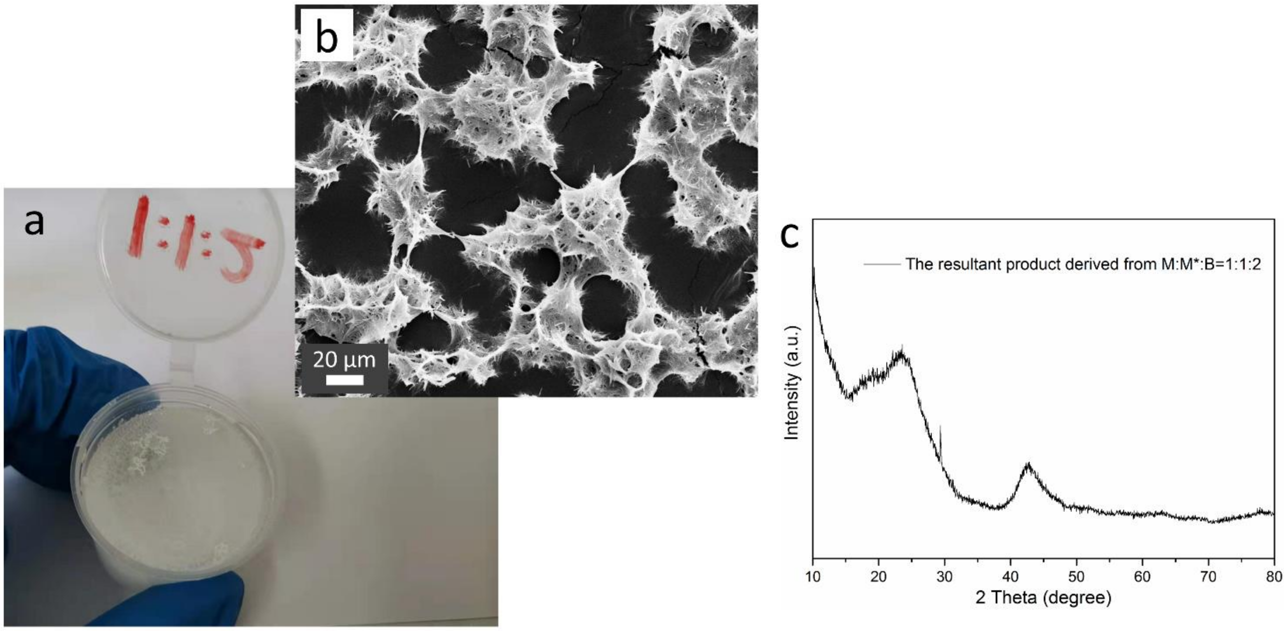

Fig. S7 (a) A photo of the supramolecular aggregates obtained at M: M*: B=1:1:2 (It can be seen that there is almost no gel formed); (b) SEM image of tiny gel fragments obtained at M: M*: B=1:1:2 ; (c) XRD pattern of the final product after the conversion process under high temperature.

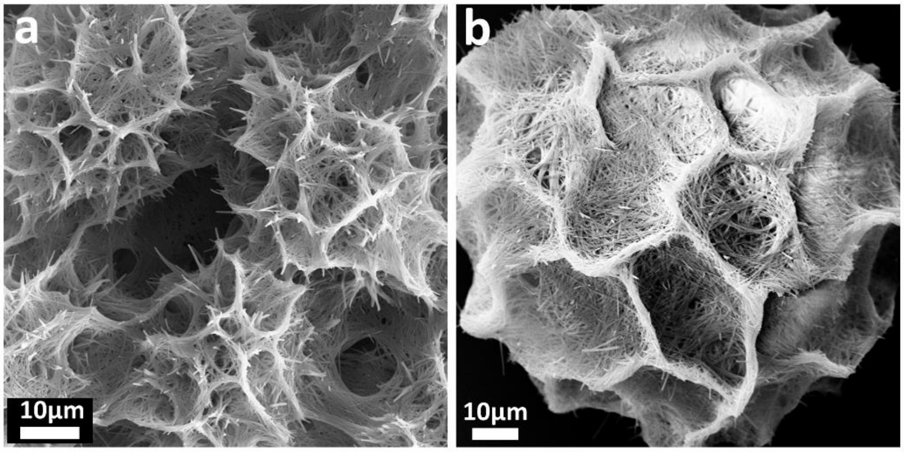

Fig. S8 SEM images of the supramolecular gels obtained at M:M*: B=1:1:6. (a) flower-like microstructure; (b) honeycomb-like microstructure.

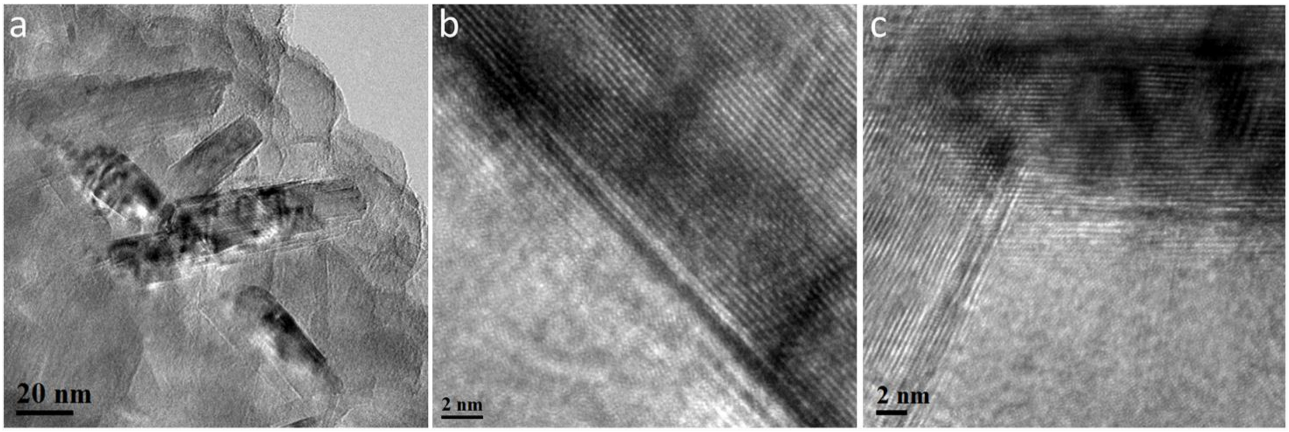

Fig. S9 TEM images of BN aerogel derived from M:M*:B=1:1:10.

Table S2 Summary of the basic information of the as-prepared BN aerogels

	BN aerogel derived from M:B=1:6	BN aerogel derived from M:M*:B=1:1:6	BN aerogel derived from M:M*:B=1:1:10
Density	28.1mg/cm^3	27.5mg/cm^3	25.7mg/cm^3
Porosity	98.8%	98.8%	98.9%

Notes for readers: There are many factors influencing the values of density and porosity. Values presented are based on samples prepared in one batch, whereas a tiny difference in experiment conditions, such as the molds you use, the way you put samples in furnace could also influence the values you get.

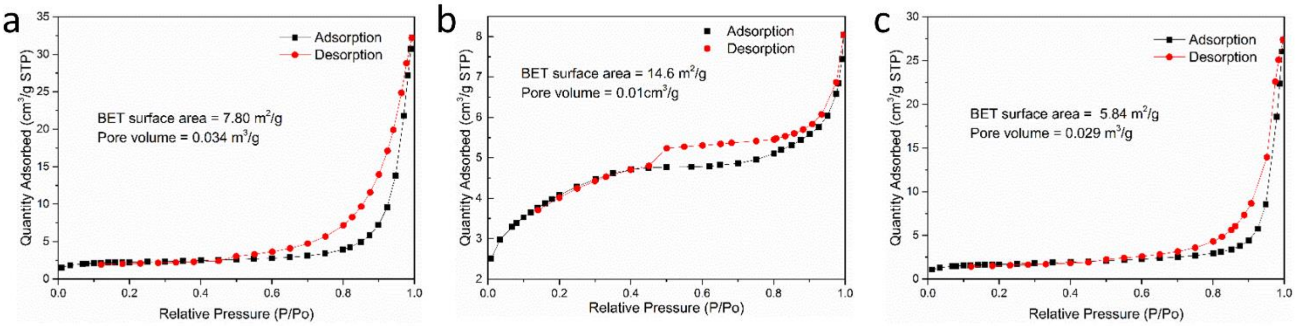

Fig. S10 N_2 sorption isotherms of the BN aerogels derived from M: B=1:6 (a), M:M*:B=1:1:6 (b), M:M*:B=1:1:10 (c). (The N_2 sorption results are also influenced by experimental conditions during sample preparation, such as atmosphere or ways of heating)

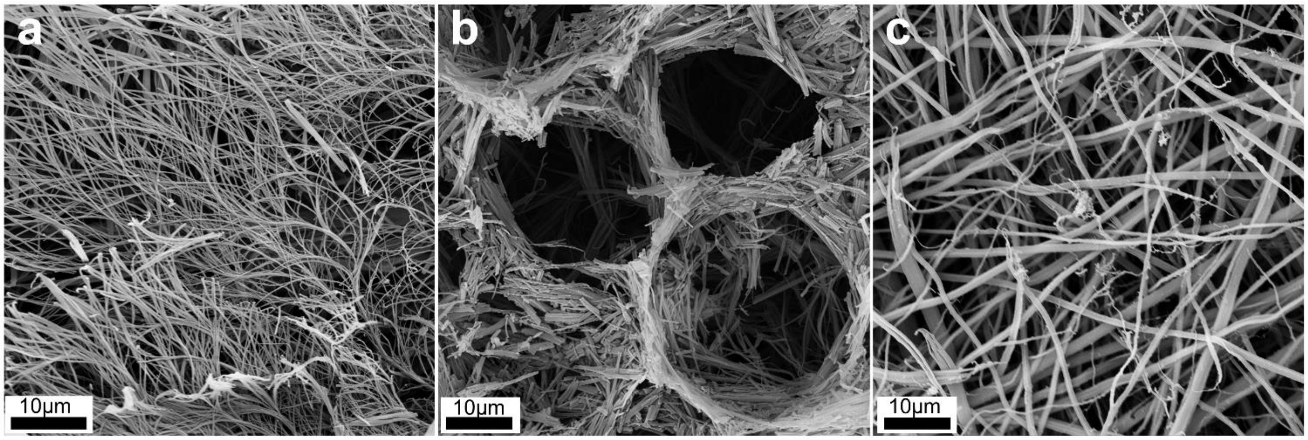

Fig. S11 SEM images of the BN aerogels derived from M: B=1:6 (a), M:M*:B=1:1:6 (b), M:M*:B=1:1:10 (c).

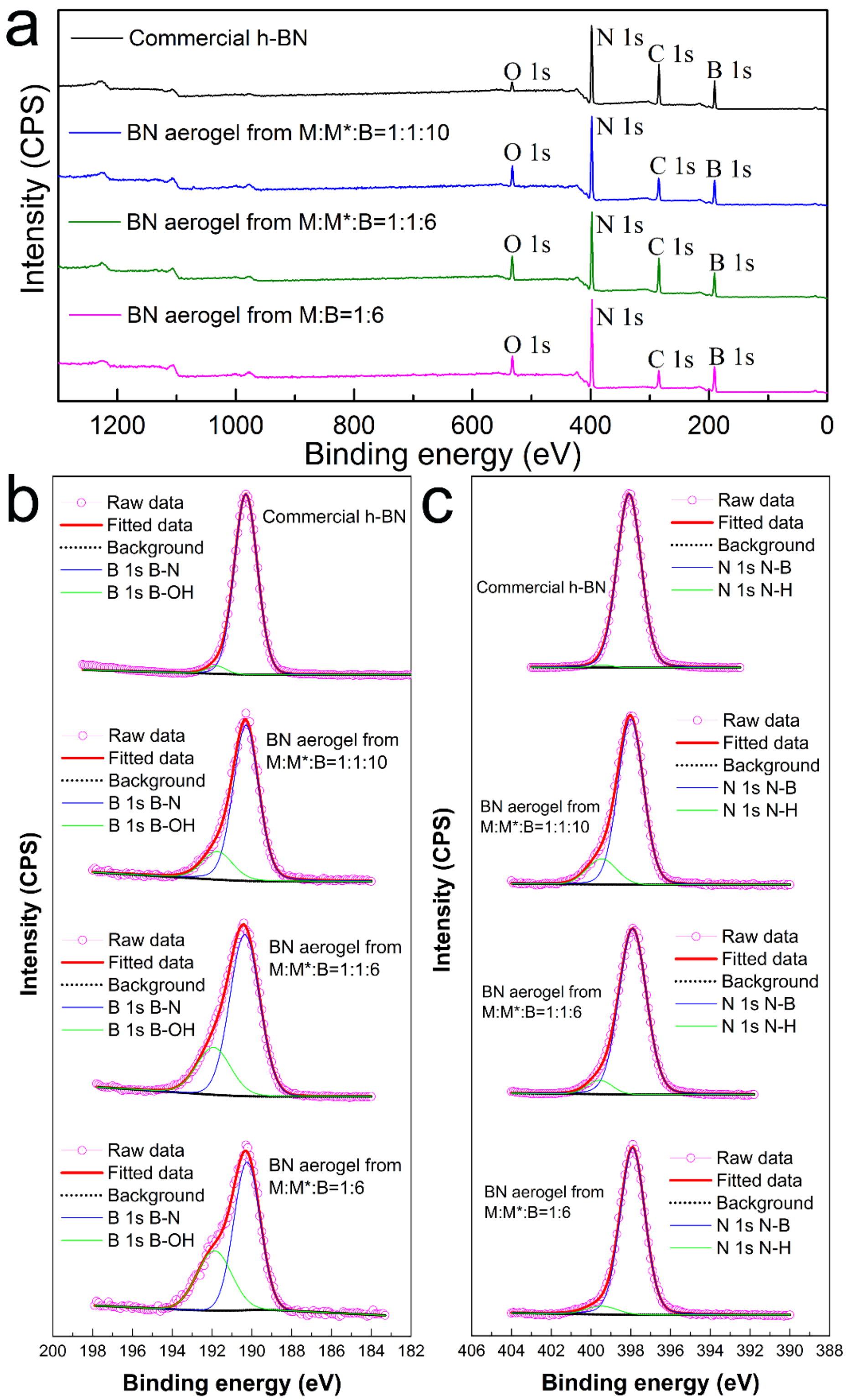

Fig. S12 XPS spectra of the as-prepared BN aerogels. (a) full survey spectra, (b) and (c) high-resolution spectra of B 1s and N 1s.

Fig. S13 Contact angle measurement of BN plates obtained by pressing BN aerogels derived from M: B=1:6 (a), M:M*:B=1:1:6 (b), M:M*:B=1:1:10 (c).

References

1. Lindquist, D.A., Borek, T.T., Kramer, S.J., Narula, C.K., Johnston, G., Schaeffer, R., Smith, D.M. & Paine, R.T. (1990). Formation and Pore Strucutre of Boron Nitride Aerogels. J. Am. Ceram. Soc. 73, 757-760.
2. Roy, B., Bairi, P. & Nandi, A.K. (2014). Supramolecular assembly of melamine and its derivatives: nanostructures to functional materials. RSC Adv. 4, 1708-1734.
3. Panicker, C.Y., Varghese, H.T., John, A., Philip, D. & Nogueira, H.I.S. (2002). Vibrational spectra of melamine diborate, C(3)N(6)H(6)2H(3)BO(3). Spectrochimica Acta Part a-Molecular and Biomolecular Spectroscopy 58, 1545-1551.
4. Atalay, Y., Avci, D., Basoglu, A. & Okur, I. (2005). Molecular structure and vibrational spectra of melamine diborate by density functional theory and ab initio Hartree-Fock calculations. J. Mol. Struc-Theochem 713, 21-26.
5. Roy, A., Choudhury, A. & Rao, C.N.R. (2002). Supramolecular hydrogen-bonded structure of a 1 : 2 adduct of melamine with boric acid. J. Mol. Struct. 613, 61-66.